

# Bulk and Surface Behavior of Cationic Guars in Solutions of Oppositely Charged Surfactants

O. Anthony, C. M. Marques, and P. Richetti\*

Complex Fluids Laboratory, CNRS/RHODIA, UMR166, Prospect Plains Road,  
CN-7500 Cranbury, New Jersey 08512-7500

Received February 18, 1998. In Final Form: July 27, 1998

We study the bulk and surface behavior of aqueous mixtures of cationic guars and anionic sulfate surfactants. The phase diagrams are determined and the phases characterized with a variety of techniques. When the surfactant is gradually added, the polyelectrolyte is physically modified by ionic binding of the surfactant or more likely surfactant aggregates to the polymer chains. This results in the increase of the solution viscosity and leads to phase separation between a polymer- and surfactant-rich phase and a dilute supernatant. Phase separation always occurs for surfactant concentrations below the critical micelle concentration (cmc). A second one-phase region is obtained for surfactant concentration as low as twice the cmc, independent of the polymer charge density or of the alkyl chain length of the sulfate surfactant. The surface behavior is investigated with a surface forces apparatus. The force profiles between two layers of cationic guar preadsorbed onto mica surfaces are measured in water and in surfactant solutions for concentrations covering the three regions of the bulk-phase diagram. We conclude that the structure of the adsorbed layers is clearly related to the structure of the corresponding polymer/surfactant mixtures.

## 1. Introduction

Mixtures of polymers and surfactants are present in a wide range of solutions for applications as divers as detergents, hair, and body care or DNA transfection. For instance, rheological properties of detergent solutions can be controlled by the incorporation of a polymer. Polymers also act as conditioners after adsorption onto hair or skin from shampoo or body-washing liquid.<sup>1–3</sup> Detergent solutions often carry polycarboxylates as sequestering agents or growth inhibitors of calcium carbonate crystal. Many natural and engineering aspects of the biological systems involve polymer–surfactant interaction. For instance, the nonviral transfection of NDA chains, a negatively charged polymer, is achieved by the formation of a complex with cationic lipids.

Such a wide range of applications has motivated many applied and fundamental studies. The bulk properties of polymer/surfactant solutions are discussed in recent review articles or monographs dedicated to the field.<sup>4,5</sup> However, the surface properties of these mixtures, a determinant factor in many of the applications, have received much less attention.<sup>6–8</sup>

In this paper we will discuss how the bulk behavior determines the interfacial structures in solutions containing polymers and surfactants of opposite charge. Three distinct regions are generally observed in the phase diagrams for oppositely charged polymer–surfactant mixtures.<sup>5,9–13</sup> At low surfactant concentrations, there is a one-phase region where an optically transparent polymer

solution solubilizes the surfactant molecules. As well-described in the literature,<sup>5,14</sup> the presence of a polyelectrolyte induces a lowering of the critical micelle concentration (cmc) of the surfactant, which is often renamed cac, critical aggregation concentration. Surfactant aggregates bind electrostatically to the polyelectrolyte chains, reducing the macromolecule charges and inducing intra- and interchain links with their aliphatic tails. Above a given, system-dependent surfactant concentration, a phase separation occurs into two distinct phases. One is dilute, while the second has a high concentration of both a polymer and surfactant. The concentrated phase is gellike, exhibiting marked viscoelastic properties. A third region can often be observed where redissolution of the polymer/surfactant complex is triggered by further addition of surfactant. The sample becomes again a clear, one-phase solution.

The solution viscosity in the first one-phase region increases as a function of added surfactant and diverges at the onset of the demixion. This is commonly attributed to a cross-linking process induced by hydrophobic self-assembly of the electrostatically bound surfactant monomers.<sup>5</sup> A similar interchain hydrophobic association is also observed in a water solution of hydrophobically modified polymers, also known as associating polymers.<sup>15</sup> The progressive redissolution of the polymer/surfactant complexes at larger surfactant concentrations is ascribed to the dressing of polymer chains with surfactant micelles.<sup>5,16</sup>

To access the influence of the phase behavior, we study with a surface forces apparatus (SFA) how a charged

(1) Goddard, E. D.; Schmitt, R. L. *Cosmet. Toiletries* **1994**, *109*, 55.  
(2) Schmitt, R. L.; Goddard, E. D. *Cosmet. Toiletries* **1994**, *109*, 83.  
(3) Weigmann, H. D.; Kamath, Y. K.; Ruetsch, S. B.; Busch, P.; Tesmann, H. *J. Soc. Cosmet. Chem.* **1990**, *41*, 379.  
(4) Goddard, E. D. *Colloids Surf.* **1986**, *19*, 255.  
(5) *Interactions of Surfactants with Polymers and Proteins*; Goddard, E. D., Ananthapadmanabhan, K. P., Eds.; CRC Press: Boca Raton, FL, 1993.  
(6) Claesson, P.; Dedinaite, A.; Blomberg, E.; Sergeev, V. G. *Ber. Bunsen-Ges. Phys. Chem.* **1996**, *100*, 1008.  
(7) Shubin, V. *Langmuir* **1994**, *10*, 1093.  
(8) Argillier, J. F.; Ramachandran, R.; Harris, W. C.; Tirrell, M. *J. Colloid Interface Sci.* **1991**, *146*, 242.  
(9) Guillemet, F.; Piculell, L. *J. Phys. Chem.* **1995**, *99*, 9201.

(10) Thalberg, K.; Lindman, B.; Karlström, G. *J. Phys. Chem.* **1991**, *95*, 3370.  
(11) Thalberg, K.; Lindman, B.; Karlström, G. *J. Phys. Chem.* **1991**, *95*, 6004.  
(12) Thalberg, K.; Lindman, B. *J. Phys. Chem.* **1989**, *93*, 1478.  
(13) Hoffman, H.; Kaestner, U.; Doenges, R.; Ehrler, R. *Polym. Eng. Networks* **1996**, *4* (5–6), 509 and references therein.  
(14) Wallin, T.; Linse, P. *J. Phys. Chem. B* **1997**, *101*(28), 5506–5513.  
(15) *Hydrophilic Polymers*; Glass, J. E., Ed.; American Chemical Society: Washington, DC, 1996.  
(16) Cabane, B.; Duplessix, R. *Colloids Surf.* **1985**, *13*, 19.

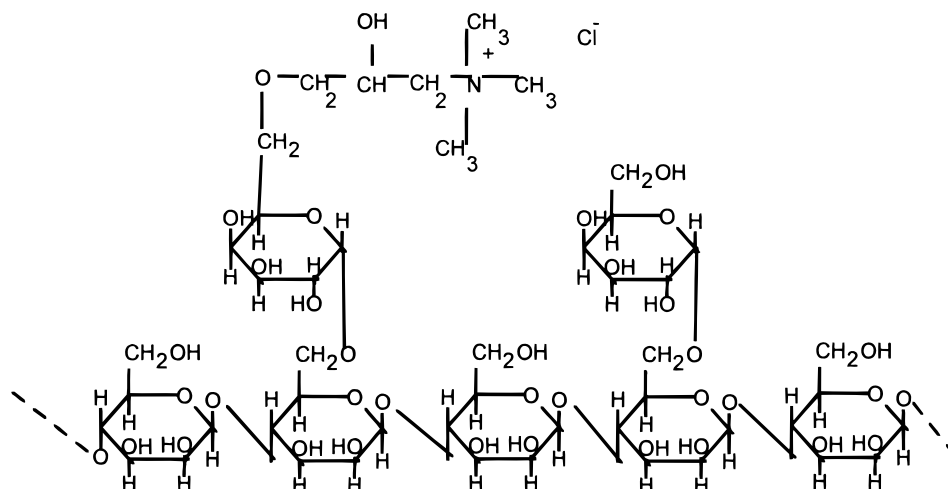


**Figure 1.** Structure of a cationic guar. The positions of the galactose units and the cationic substituents are randomly distributed.

polymer layer adsorbed on an immersed solid surface is modified by progressive addition in the solution of an oppositely charged surfactant. The polymer adsorbed layer is exposed to a surfactant solution with surfactant concentrations spanning the three regions of the bulk-phase diagram. The polyelectrolyte under investigation is a modified natural polysaccharide, a cationic guar while the anionic surfactant is the sodium dodecyl sulfate. The unmodified neutral guar is a water-soluble polymer, thus avoiding speculation on whether the phase separation is induced by a reduction of the overall charge on the chains or whether redissolution at larger surfactant concentrations proceeds by a charge-reversal mechanism. These two important possibilities must be considered when the polyelectrolyte backbone has poor solubility.

The paper is organized as follows. In section 2, we describe the materials and the experimental techniques used in this work. Section 3 is devoted to the experimental results. The phase diagrams and a detailed characterization of each phase domain are presented, followed by a description of the force profile measured between two mica surfaces covered by the cationic guar layer adsorbed from a free surfactant solution. The evolution of the force profiles as a function of the surfactant concentration is then presented. Section 4 consists of the discussion. The final section highlights the main conclusion of the study and sketches some perspectives.

## 2. Experimental Section

**2.1. Materials.** Cationic guars were supplied by Rhône-Poulenc. The regular guar is a galactomannane polysaccharide. The backbone of the polymer is constituted of mannose sugar units, which bear some randomly distributed galactose units. A schematic representation of its chemical structure is given in Figure 1. The ratio mannose/galactose is close to 2 (see ref 17). The molecular weight was measured by GPC and was estimated at about  $2.3 \times 10^6$  g/mol, independent of the degree of cationic modification. No polymer aggregates have been evidenced with this technique. For the natural guar, that is, the uncharged polymer, the overlap concentration has been measured at  $C^* = 0.14$  wt %. Cationic guars were obtained by grafting hydroxypropyl trimethylammonium chloride groups both on mannose and galactose units. The charges are believed to be randomly distributed along the chains. In the present study, we have used four cationic guars of different charge density. The degree of cationic substitution, determined by nitrogen analysis, has been found to be 4%, 14%, 20%, and 30% respectively for the samples that we will call hereafter G4, G14, G20, and G30. The specific

cationic guar G14 has a charge rate of 14% which means there is a positive charge on approximately one out of every seven sugar units. The guar sample stocks have been purified according to the complete procedure provided by Dr. A. Goswami from Rhodia North America. This purification is performed in order to remove the insoluble compounds and the borate ions.

Sodium dodecyl sulfate, SDS (>99%), was obtained from Fluka and was purified by recrystallization from ethanol. However, sodium decyl sulfate, SdS, was homemade while sodium tetradecyl sulfate, STS, was obtained from Merck and used as received. The salts were high-purity grade supplied by Aldrich. The sample of purified pyrene was graciously provided by Dr. R. Zana and has the same origin as the samples used in ref 18.

**2.2. Methods.** All experiments were performed at room temperature (25 °C). For the determination of the phase diagrams, the samples were prepared from stock solutions of a surfactant and polymer and gently shaken in order to avoid the formation of foam. They were then left to equilibrate and sediment for several days. To detect any bacterial degradation of the natural polysaccharide polymer in solution, regular viscoelastic tests have been carried out with gel solutions. Over a period of 10 days, no significant changes have been observed for the same sample.

The viscosity measurements of polymer/surfactant mixtures were performed using a Rheometrics Ares rheometer, in double-wall geometry. Hereafter, the presented viscosity values correspond to the Newtonian plateau extrapolated at zero shear rate.

The fluorescence measurements were made with a spectrofluorimeter Hitachi F4010. The fluorescence spectrum of pyrene exhibits five vibronic peaks. The ratio of the intensities of the first and third peaks varies with the polarity of the medium surrounding the pyrene probe.<sup>19,20</sup> The  $I_1/I_3$  ratio is high in a polar medium (1.87 in water), low in an apolar medium (0.66 in cyclohexane), and intermediate in micellar media (1.2 in SDS micelles).

Some time-resolved fluorescence quenching (TRFQ) experiments have been performed at Strasbourg in the laboratory of Dr. R. Zana. This technique, allowing for the determination of the micelle aggregation number, has been widely described in the literature.<sup>20</sup>

The force measurements were performed using an interferometric surface forces apparatus (SFA),<sup>21</sup> model Mark IV<sup>22</sup> with a chamber volume of about 40 cm<sup>3</sup>. This device allows for the measurement of forces between two muscovite mica sheets glued

(18) Binana-Limbélé, W.; Zana, R. *Macromolecules* **1990**, *23*, 1731.

(19) Kalyanasundaram, K.; Thomas, J. K. *J. Am. Chem. Soc.* **1977**, *99*, 2039.

(20) Zana, R. *Surfactant Solutions: New Methods of Investigation*; Zana, R., Ed.; Plenum Press: New York, 1987; Chapter 5.

(21) Israëlachvili, J. N.; Adams, G. E. *J. Chem. Soc., Faraday Trans. I* **1978**, *74*, 975.

(22) Parker, J. L.; Christenson, H. K.; Ninham, B. W. *Rev. Sci. Instrum.* **1989**, *60*, 3135.

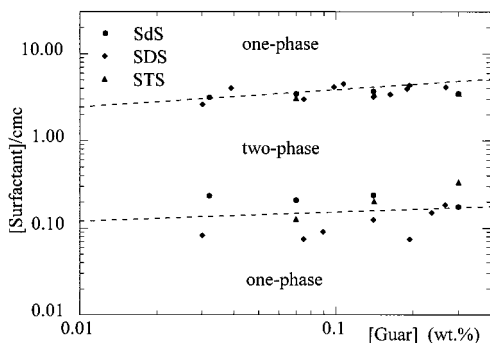


**Figure 2.** Phase diagram of three G14/sodium alkyl (decyl, dodecyl, and tetradecyl) sulfate systems. The surfactant concentration is given as a fraction of each surfactant cmc. The displayed points indicate the boundaries of the one-phase regions.

onto optical cylindrical lenses mounted in crossed cylinder geometry. The force is measured as a function of the separation  $D$  between the two surfaces. At the beginning of each experiment, the surfaces are brought together until the contact in air allows us to determine the zero separation of force profiles as the contact position between the two bare mica surfaces. We always achieved the adsorption of guar as follows. A 0.042 wt % (weight percent) solution of cationic guar was introduced in the chamber and left overnight for adsorption. The solution was then removed and replaced several times by pure water, to remove the nonadsorbed polymer. When the chamber was emptied, a drop of water was always maintained between the two surfaces, such that the adsorbed layers never dried. A low concentration salt solution ( $\text{NaNO}_3$  at  $3 \times 10^{-4}$  M) was finally introduced in the chamber. After the thermal equilibrium is achieved, the interaction forces between the surfaces were measured at least three times. The salt solution was then replaced by SDS solutions of increasing concentration.

### 3. Results

**3.1. Phase Diagrams.** Figure 2 compares the phase diagrams of G14 guar mixed with anionic surfactants having the same polar head but alkyl chains of different lengths. The log-log scale has been chosen in order to more clearly show the precipitation lines at low surfactant concentrations. The surfactants are sodium decyl, dodecyl, or tetradecyl sulfate (SdS, SDS, and STS). The surfactant concentration has been normalized by their critical micellar concentration (cmc), measured in the absence of a polymer, respectively  $3.25 \times 10^{-2}$ ,  $8.1 \times 10^{-3}$ , and  $2.0 \times 10^{-3}$  M.

All the mixtures follow the same generic scenario for water solutions of oppositely charged polyelectrolyte/surfactant mixtures.<sup>5,10-12</sup> Three regions are observed, depending on the surfactant concentration. At a given guar concentration, when the surfactant concentration is increased from zero (first monophasic regime), the solution becomes more and more viscous and visually viscoelastic. For intermediate surfactant concentrations, phase separation is obtained in agreement with the literature.<sup>5,9</sup> The solutions then turn to be turbid and some white flakes develop. After equilibration, a macroscopic separation in two distinct phases is achieved. The bottom phase looks like a gel. For higher surfactant concentrations, a gradual redissolution is obtained, and at a given concentration the whole gel is finally redispersed. As in other investigations,<sup>9</sup> the onsets of phase separation and redissolution increase slightly with the polymer concentration (see Figure 2).

It is interesting to notice that the redissolution always occurs at very similar fractions of the cmc (Figure 2), almost independently of the hydrophobicity of the surfactant in the series of the sodium alkyl sulfates. Here-

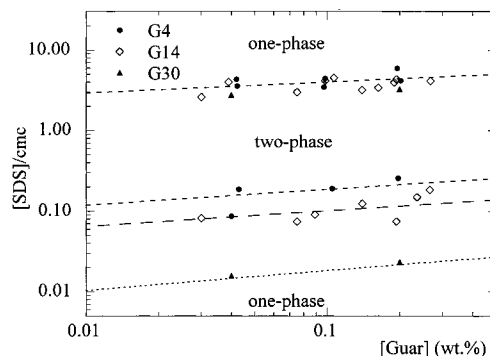


**Figure 3.** Phase diagram of three cationic guar (G4, G14, and G30)/SDS systems. The SDS concentration is given as a fraction of cmc. The displayed points indicate the limits of the one-phase regions.

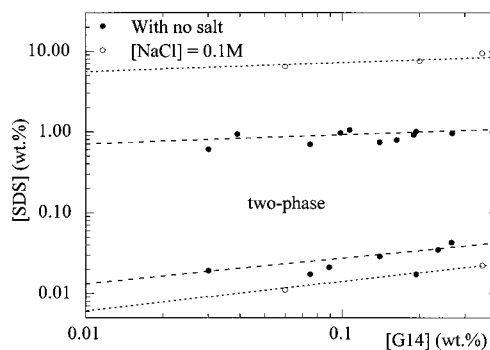


**Figure 4.** Phase diagram of the G14/SDS system in the presence and absence of 0.1 M NaCl. The displayed points indicate the limits of the one-phase regions.

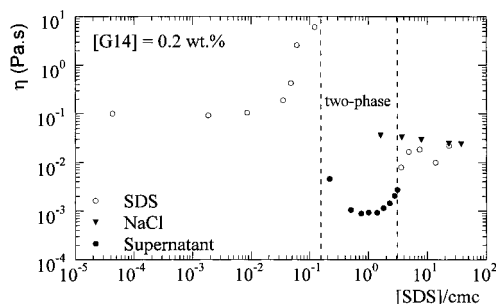
after, all the surfactant concentrations will be given as a fraction of the cmc. The same trend is seen for the phase-separation boundary. The data are more scattered here but no systematic variation is observed from one surfactant to another after being normalized by the cmc. This suggests that this phase limit also scales with the cmc, as already reported in ref 12.

Figure 3 is a comparison of phase diagrams established for three cationic guar, respectively, G4, G14, and G30, of different charge density, mixed with SDS. Phase separation is obtained for the three systems. Note that the redissolution line is completely independent of the charge rate of the polymer within the experimental accuracy. Also, the increase of the charge density lowers the onset of precipitation.

The effect of the ionic strength on the position of the coarsening and redissolution lines has been tested. As shown in Figure 4, the addition of 0.1 M NaCl lowers the onset of phase separation and leads to an increase of the surfactant amount necessary to redissolve the gellike phase. This behavior is in disagreement with previous results.<sup>12</sup> This point will be discussed further.

**3.2. Phase Characterization.** As mentioned above, the addition of an anionic surfactant to a cationic guar solution modifies the viscosity of the system, in both one-phase regions.

Figure 5 displays the evolution of the Newtonian viscosity for a 0.2 wt % G14 solution as a function of the SDS concentration. One can see, on one hand, that the presence of less than 0.01 cmc of SDS does not modify significantly the viscosity of the polymer solution. On the other hand, for higher SDS concentrations, the viscosity increases sharply at the onset of the demixion line, reaching a value about 100 times higher than the



**Figure 5.** Newtonian viscosity of G14/SDS and G14/NaCl mixtures. The viscosity measured in the two-phase region corresponds to the supernatant.

initial value. After redissolution, the viscosity is almost constant and about 5 times smaller than the viscosity of the pure polymer solution. For the sake of comparison, we have reported in Figure 5 the viscosity of a same G14 polymer solution, with no surfactant but with equivalent salt concentrations. One can already note the similarity of values.

Complementary to this, we have also measured the viscosity of the supernatant in the two-phase region (● in Figure 5). Interestingly, a minimum is observed for a SDS concentration corresponding to the cmc. At this minimum, the viscosity is only 10% higher than the value measured for pure water, suggesting strongly that most polymers are in the decanted phase. We do not explain why this maximum of phase separation occurs for a SDS concentration equivalent to the cmc.

For SDS concentrations higher than the cmc, the viscosity of the supernatant increases rapidly, indicating a progressive redissolution of the precipitate.

The minimum in the viscosity of the supernatant is in qualitative agreement with the titrations and the elementary analysis carried out in both phases, that is, the gellike phase and the liquid phase. Two regimes can be distinguished. For a 0.2 wt % G14 guar solution, the first regime stretches out from the separation line (0.22 cmc) to the cmc while the second one extends from the cmc to the redissolution line (3 cmc).

In the first concentration range, we have found that the mass of the dried gel phase increases, reaching a maximum at the cmc. About  $\frac{9}{10}$  of the guar is then in the gellike phase. Moreover, analysis of the gel phase shows that the ratio  $R$  between the number of surfactant ions and polymer charge is fairly constant in the first concentration domain.  $R$  varies between 1 and 1.5. Previous studies addressing other complexes of polyelectrolytes/oppositely charged surfactants mention similar values for  $R$ , with however a dependence on the charge rate of the polymer.<sup>5,23</sup>

In the second concentration range, the fraction of guar in the gellike phase decreases gradually upon an increase of the surfactant concentration, while  $R$  increases rapidly from 1.5 to more than 5.

The spectrofluorimetry results are presented in Figure 6. The ratio between the intensities of the first and third peaks of the fluorescence spectrum of pyrene is plotted as a function of the surfactant concentration. This ratio is related to the polarity of the medium where the pyrene probes are solubilized. The results indicate that, in the presence of 0.1 wt % G14 guar, the  $I_1/I_3$  ratio starts to decrease for a SDS concentration close to 0.01 cmc, the concentration where the viscosity starts to increase. This value could then be a good estimation of the critical aggregation concentration, above which the surfactant

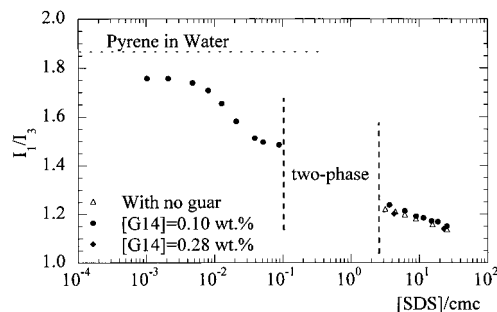


**Figure 6.** Ratio between the first and third peak of the fluorescence spectrum of pyrene in G14/SDS solutions.

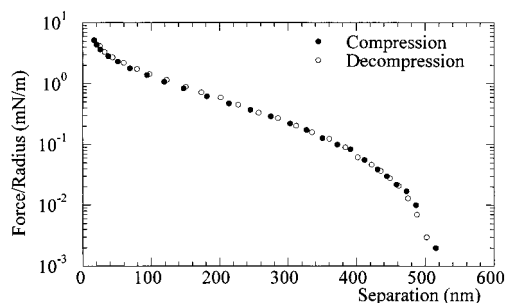


**Figure 7.** Force profile between two mica surfaces coated with G14 guar, in the absence of the surfactant. Both data obtained compression and decompression are displayed.

aggregates to the polymer. The  $I_1/I_3$  ratio decreases quite rapidly, as is the case when aggregates of the surfactant are formed onto the polymer.

For high surfactant concentrations, in the second monophasic region, the fluorescence technique does not allow one to distinguish between bound and free micelles. Indeed, the  $I_1/I_3$  ratio of equivalent micellar solutions is not modified by the presence of guar at different concentrations, as exemplified in Figure 6, indicating that the polarities probed by the pyrene are equivalent. On the same hand, time-resolved fluorescence quenching measurements give aggregation numbers of about 60 for 3 cmc SDS solutions, independent of the presence of G14 guar.

**3.4. Surface Forces Measurements.** **3.4.1. Adsorption of Cationic Guar.** We present in Figure 7 the force profile measured between two mica surfaces, after adsorption of the G14 polymer onto the mica sheets. The force profile has been obtained in a weakly salted water solution ( $[\text{NaNO}_3] = 3 \times 10^{-4} \text{M}$ ), in the absence of any surfactant and polymer in the solution, after extensive rinsing with pure water has removed the initial guar solution used for the adsorption. The profile is highly reproducible, independent of the probed surface position and of the number of compression and decompression runs performed on a same position. The compression and decompression runs are very similar and always repulsive. The most striking aspect of this profile is its very long range, about 480 nm, which means that on average an adsorbed layer has a thickness of about 240 nm.

In Figure 8, we have collected the force profiles measured with adsorbed guars of different charge density, respectively, G4, G14, and G30. The experimental procedure for measuring of the force profiles with adsorbed G4 and G30 was similar to the previous one used with G14. The layers were also adsorbed from 0.042 wt % polymer solutions. Similarly, these force profiles have been obtained with coated micas immersed in a weakly salted water solution, free of any surfactant and polymer, resulting from repeated rinsing. The range of the profile

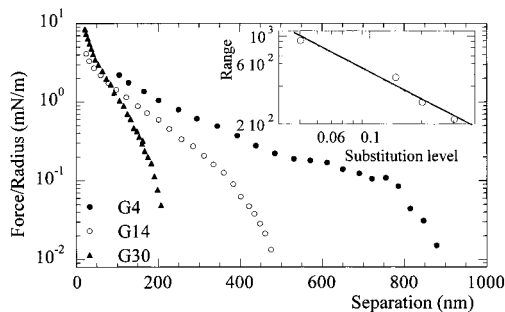


**Figure 8.** Force profiles between two mica surfaces coated with G4, G14, and G30 guar, in the absence of the surfactant. Only data obtained on compression are shown. The insert displays the range of the force as a function of the charge degree.

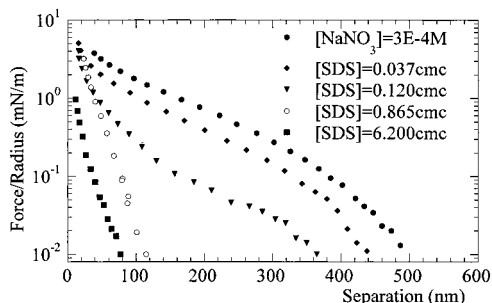


**Figure 9.** Force profiles between two mica surfaces coated with G14 guar, in SDS solutions of different concentrations. Only data obtained on compression runs are displayed.

is very dependent on the charge rate. The higher the rate, the shorter the range. For instance, with the G4 coating, the range is almost double (900 nm), compared to the range obtained for G14 (480 nm). This behavior may express the weakening of the attractions between the polymer and the surface, allowing the polymer to adopt a more extended conformation. Incidentally, a higher charge rate stretches a polymer in bulk and decreases the length of the loops when the polymer is adsorbed on the surface. In the insert of Figure 8, we have reported in a logarithmic scale the evolution of the force range as a function of the charge density. A fourth guar has been studied here, G20, with a degree of cationic substitution of 20%. From the plot, we can extract an exponent close to  $-0.7$ .

In the following paragraph, we discuss how the preadsorbed polymer layers are modified when the water is replaced by a surfactant solution.

**3.4.2. Addition of SDS to a Preadsorbed Guar Layer.** Figure 9 shows the evolution of force profiles between the mica surfaces precoated with G14 guar, in SDS solutions of different concentrations. Since compression and decompression runs are fairly similar at all surfactant concentrations, only the compression runs are plotted in Figure 9 for the sake of clarity.

Weakly salted water has been replaced first by very dilute SDS solutions, free of polymers, respectively 0.037 cmc (◆) and 0.12 cmc (▼). According to the bulk-phase diagram, Figure 2, we can assume that the adsorbed guar layer would be in the first one-phase region, below the phase-separation line. As shown in Figure 9, the range of the forces decreases slightly from about 480 to 380 nm, still a large value.

For a surfactant concentration of 0.865 cmc, the phase diagram, Figure 2, shows that a G14–SDS mixture is in the two-phase region. With the same surfactant solution (○) in the SFA, we have measured a dramatic decrease of the range of the forces, down to about 130 nm (Figure

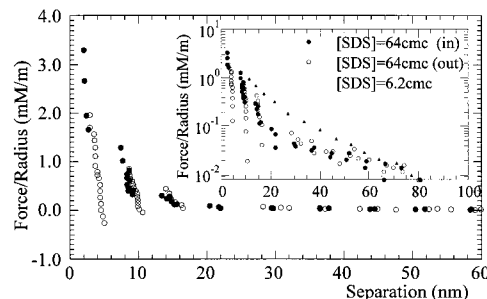


**Figure 10.** Force profile between two mica surfaces coated with G14 guar, in a 64 cmc SDS solution. Both data obtained on compression (IN) and on decompression (OUT) are displayed. The compression force profile obtained in a 6.2 cmc SDS solution is also shown.

9). The conformation of the adsorbed polymer has completely changed. According to the bulk-phase diagram, we might suggest that the adsorbed layers have collapsed into denser structures. For this particular solution, the decompression and compression runs do not overlap so well. At small separations, the force profile appears to be slightly steeper when the surfaces are separated, as a weak extra attractive force is induced after compression. We have not, however, been able to consistently reproduce this weak behavior.

According to the bulk-phase diagram, the introduction of a new solution in the SFA at a concentration standing above the redissolution line, Figure 2, would lead to a reswelling of the adsorbed layers. We have measured the force profiles at such concentrations, after having induced the collapse of adsorbed layers with lower surfactant concentration solutions. With a 6.2 cmc SDS solution, for instance, as illustrated in Figure 9 (■) we do not observe any swelling of the adsorbed layers. The range of the forces even decreases slightly down to 100 nm. However, it is noteworthy that the separation corresponding to a similar applied load at the maximum compression has become smaller (11 nm), when it was fairly constant (about 20 nm) for the previous lower SDS concentrations. This means that either the configuration of the adsorbed layers is even flatter or that a part of the adsorbed polymer has been removed from the surface, desorbed by SDS micelles.<sup>24</sup> The compression and decompression runs are well-superimposed.

Finally, with a concentrated SDS solution (64 cmc), the force profile exhibits new features as illustrated in Figure 10. Oscillatory profiles are now obtained both in compression and decompression, indicating a layering of SDS micelles in the neighborhood of the surfaces.<sup>6,25</sup> The compression (●) leads to a successive depletion of the layers; however, the decompression (○) allows the inclusion of micelles, layer by layer. Moreover, the separation at the maximum compression has decreased dramatically. Indeed, we were able to easily reach separations as small as 2 nm, suggesting strongly that only a few polymer chains remain adsorbed. However, we believe that some polymers are still present since a weak long-range repulsion is still measured at larger separations. On average, despite oscillations, the measured force is repulsive with a range close to 80 nm as displayed in the insert of Figure 10. Only the last oscillation, before the contact, has a minimum within a negative force domain. Note also that the background of this profile is not very different from the one obtained with the 6.2 cmc solution (△) as shown in the log plot insert.

(24) Shubin, V.; Petrov, P.; Lindman, B. *Colloid Polym. Sci.* **1994**, *272*, 1590.

(25) Richetti, P.; Kekicheff, P. *Phys. Rev. Lett.* **1992**, *68*, 1951.

#### 4. Discussion

**4.1. Phase Behavior.** In general, three driving forces rule the binding of ionic surfactants to oppositely charged polymers:

(1) The most obvious interaction is the electrostatic attraction between the opposite charges of the polymer and the surfactant. Therefore, the binding sites are the polymer charges.<sup>23,26,27</sup>

(2) The hydrophobic attractions between the surfactant tails may result in a cooperative binding of the surfactant to the polymer.<sup>5,28,29</sup> This effect is favored by short distances between the binding sites on the polymer, as observed for polyacrylates and other polyelectrolytes whose charge rate can be tuned.<sup>23,26</sup> With a cooperative process, a critical aggregation concentration (cac) lower than the surfactant cmc is observed. Bound micelles or "aggregates" develop then along the polymer chains.

(3) Strong hydrophobic attractions between the polymer and surfactant are observed when the polymer itself bears enough hydrophobic parts already being able to make hydrophobic microdomains, in the absence of a surfactant.<sup>30,31</sup> This process may completely dominate the previous ones. The binding becomes then noncooperative or even anticooperative since the attractions between surfactants do not control the binding. A cac is never observed in such systems. At a low surfactant concentration, almost all of the surfactant is then bound to the polymer.<sup>30</sup> However, since the binding is noncooperative, no new hydrophobic microdomains are created.

For our mixtures, the main driving force is undoubtedly the electrostatic interaction between the opposite charges of both components. Collective binding is unlikely to occur along one polymer chain. The studied guars have relatively long distances between charges, and the mean separation is of the same order or larger than the surfactant molecule length. For instance, the mean distance between two charges along a G14 chain is about 2.5 nm, roughly the length of two stretched SDS molecules. Since our cationic guars bear no hydrophobic parts, the third process can be definitively ruled out, even if the fluorimetry results indicate that the studied guars are able to protect slightly the pyrene probes (Figure 6).

At a low surfactant concentration, we expect the formation of surfactant aggregates, most of them being bound to several polymer chains. This behavior has been observed in polyelectrolyte/oppositely charged surfactant systems.<sup>13,32</sup> The decrease of the  $I_1/I_3$  ratio in the first one-phase domain (see Figure 6) indicates that surfactant aggregates already exist at a low surfactant concentration. However, they appear to be small, as suggested by the still relatively high value of  $I_1/I_3$  even close to the precipitation line ( $I_1/I_3 = 1.48$ ). In these small aggregates, the pyrene probes would only be partly shielded from the water environment. An alternative explanation for such a high ratio would be that only a fraction of the pyrene is solubilized in the small amount of available hydrophobic microdomains. Preliminary aggregation number measurements performed with time-resolved fluorescence

quenching indicate that those aggregates would involve less than 25 surfactant molecules.

Intermacromolecular associations are more likely to occur when the polymer concentration is above the overlapping concentration  $C^*$ . These associations result in a progressive gelification of the soluble polymers upon addition of SDS, as clearly revealed by the viscosity measurements.<sup>13</sup> The ultimate stage of this association process is a phase separation observed for surfactant concentrations always lower than the cmc as displayed in Figures 2 and 3.

The emergence of a two-phase region has been frequently reported in the literature for mixtures of polymers and surfactants of opposite charges.<sup>10–12,33–36</sup> It is well-established that, in the absence of added salt, associative phase separation is obtained<sup>5</sup> for a surfactant concentration lower than the cmc of the pure surfactant. The onset of precipitation appears to depend both on the polymer charge rate<sup>12</sup> and on the hydrophobicity of the surfactant.<sup>11</sup> A decrease of the hydrophobicity of the surfactant results in a reduction of the area of the two-phase region. Redissolution is also more difficult to achieve for highly charged polyelectrolytes.<sup>5</sup> It is of interest to note that the maximum turbidity has also been obtained for a stoichiometric mixture of opposite charges.<sup>37</sup>

As shown in Figure 2, the position of the precipitation and redissolution lines for the G14/sodium alkyl sulfate systems almost coincide once the surfactant concentrations have been normalized by their cmc's. No direct correlation is observed between the charge neutralization and the precipitation process. For a polymer concentration of 0.2 wt %, the mixture separates upon addition of 4.4 SdS, 1 SDS, or 0.4 STS molecules per polymer charge (but these surfactant amounts are not necessarily bound to the polymer). Furthermore, for the same polymer concentration, coarservation is observed when approximately 6, 1, and 0.1 SDS molecules are added per G4, G14, and G30 charge, respectively. The fact that the G30 polymer phase separates when 0.1 SDS molecule is added per polymer charge clearly demonstrates that the macroscopic charge neutralization is not required to induce phase separation. For our guar mixtures, the phase separation does not correspond to the onset of insolubility of single chains, but more likely to strong hydrophobic attractions between the polymer chains. Consequently, it is not really surprising that the precipitation lines scale with the cmc of the surfactants which is also ruled by the hydrophobic attractions between the surfactant molecules.

Guillemet and Piculell<sup>9</sup> consider that the redissolution occurs at a fixed value of the binding ratio  $\beta$ , defined as the ratio between the bound surfactant concentration and the concentration of polymer charges. This assumption leads for the redissolution line to the following equation:

$$C_{\text{tot}} = C_{\text{free}} + \beta C_{\text{pol}} \quad (1)$$

where  $C_{\text{tot}}$  is the total concentration of surfactant required to redissolve the system,  $C_{\text{free}}$  is the free surfactant concentration at redissolution, and  $C_{\text{pol}}$  is the polymer charges concentration. They obtain a value of  $\beta$  increasing with the salt concentration,<sup>9</sup> and a value of  $C_{\text{free}}$  lower than the cmc of the SDS. For the guar/SDS system, we

(26) Shimizu, T. *Colloids Surf.* **1994**, *84*, 239.

(27) Kiefer, J. J.; Somasundaran, P.; Ananthapadmanabhan, K. P. *Langmuir* **1993**, *9*, 1187.

(28) Hayakawa, K.; Kwak, J. C. T. In *Cationic Surfactants: Physical Chemistry*; Ribing, D., Holland, P., Eds.; Marcel Dekker: New York, 1991; p 189.

(29) Thalberg, K.; Lindman, B. *Colloid Surf. A* **1993**, *76*, 283.

(30) Anthony, O.; Zana, R. *Langmuir* **1996**, *12*, 3590.

(31) Benrraou, M.; Zana, R.; Varoqui, R.; Pefferkorn, E. *J. Phys. Chem.* **1992**, *96*, 1468.

(32) Petet, F.; Audebert, R.; Iliopoulos, I. *Colloid Polym. Sci.* **1995**, *273*, 777.

(33) Piculell, L.; Lindman, B. *Adv. Colloids Interface Sci.* **1992**, *41*, 149.

(34) Dubin, P. L.; Oteri, R. *J. Colloid Interface Sci.* **1983**, *95*, 453.

(35) Leung, P. S.; Goddard, E. D. *Colloids Surf.* **1985**, *13*, 47.

(36) Ananthapadmanabhan, K. P.; Leung, P. S.; Goddard, E. D. *Colloids Surf.* **1985**, *13*, 63.

(37) Harada, A.; Nozakura, S. *Polym. Bull.* **1984**, *11*, 175.

found that  $C_{\text{tot}}$  is independent of the polymer charge rate (see Figure 3). It would then be inaccurate here to use the polymer charge concentration for  $C_{\text{pol}}$ . We replace it by the total polymer concentration, expressed in weight percent. With these parameters, the linear eq 1 is then in very good agreement with the redissolution line, giving the following numerical values:  $C_{\text{free}} = 2.3$  cmc and  $\beta = 5.3$  cmc/polymer wt %. Such a value for  $\beta$  means that the bound surfactant concentration is equivalent to 5.3 cmc (0.043 M) for a polymer concentration of 1 wt % at the redissolution. Therefore, on average, 5.6 surfactant molecules are bound per polymer charge, indicating that aggregates of the surfactant are now linked to the polymer. Of course, we are unable to discuss the real size of these aggregates; however, they are probably bigger than suggested by the above value. Presumably, some polymer charges do not bear any aggregate, and some aggregates might be linked to several polymer charges.

As previously mentioned, the polymer charge rate and the hydrophobicity of the surfactant do not affect the  $C_{\text{free}}$  value. At redissolution, we found a concentration of 2.3 cmc for all our cationic guar/sodium alkyl sulfate systems. Therefore, free micelles are always present before the complete redissolution. According to our knowledge, no model exists to explain such a result. During the redissolution process, two hydrophobic associations compete, the initial one, leading to polymer/polymer gelation, and a new one, proceeding to polymer/micelle complexes. This might explain why no rapid decrease of the viscosity is then observed at the redissolution, as has been reported when the free surfactant concentration is lower than the cmc.<sup>9</sup> When redissolution is completed, the polymer chains would already be partially saturated by the surfactant aggregates, and therefore they would adopt a less extended conformation as will be discussed below.

A linear fit also describes well the coascervation line: the intercept gives now the free surfactant concentration while the slope  $\beta$  measures the amount of bound surfactant required to trigger the phase separation. For the G14/SDS system, we obtain a free surfactant concentration of about 0.085 cmc while  $\beta$  is close to 0.5 cmc/guar wt %. The last value suggests that  $8 \times 10^{-4}$  M of surfactant would be bound for a guar concentration of 0.2 wt %, corresponding to  $1.5 \times 10^{-3}$  M charges. The phase separation is initiated when approximately half the polymer charges present in solution bind a surfactant. This does not mean, however, that the composition of the precipitate reflects the average composition of the solution.

In the literature, addition of salt is quoted as often reducing or even suppressing the two-phase region.<sup>11</sup> Increasing the ionic strength shifts the cac to higher values.<sup>5,18,28</sup> When phase separation is still observed, it occurs at larger surfactant concentrations. Shortening of the electrostatic attraction range is the invoked reason. In some particular cases, when the polymer is hydrophobically modified, the addition of salt may conversely result in a lowering of the onset of precipitation (salting out effect). Indeed, the solubility of the hydrophobic moieties decreases when the ionic strength increases. This behavior occurs especially when the polymer backbone is intrinsically water-insoluble. However, the position of the redissolution line seems to depend less on the salt concentration.<sup>9</sup>

With a pure G14 guar solution, the addition of NaCl up to 2 M does not induce any phase separation, attesting that the guar is intrinsically water-soluble with or without charges. In the presence of a surfactant, a salt effect is expected since the phase separation is caused by hydrophobic attractions between bound surfactants along guar

chains. These attractions are known to become stronger in the presence of salt. Therefore, a lower binding rate is required to induce the demixion. This effect is shown in Figure 4. The phase transition occurs at lower surfactant concentrations in the presence of salt. The linear fit of the coascervation line then that obtained for a 0.1 M NaCl salted mixture indicates that the free surfactant concentration has slightly decreased: 0.06 cmc against 0.085 cmc in the absence of salt. Also, the corresponding concentration of bound surfactants becomes smaller: 0.2 SDS/polymer charge against 0.5 SDS/polymer charge in the absence of salt. Note that we do not recover a factor of 4 that would correspond to the reduction of the SDS cmc upon addition of 0.1 M NaCl salt.

A linear fit of the redissolution line in the presence of 0.1 M NaCl has also been carried out. We found that, at the redissolution, the free surfactant concentration is equal to about 23 cmc ( $\text{cmc} = 8.1 \times 10^{-3}$  M) and that an average of 41 SDS molecules are bound at every polymer charge. This means that about 90% of the weight of the polymer/surfactant complex is due to the surfactant. Both free and bound surfactant concentrations are thus considerably increased upon the addition of salt, 23 cmc and 41 SDS molecules instead of 2.3 and 5.6, respectively, with no salt. Note that these results are in contradiction to published results<sup>9</sup> where lower amounts of surfactant are found to induce the redissolution in the presence of salt.

Beyond the redissolution concentrations, upon a further increase of the surfactant concentration, a progressive decrease of the solution viscosity is generally reported in the literature.<sup>9,38</sup> The admitted interpretation is that the amount of polymer chains in contact with the same aggregate decreases since the number of bound aggregates increases with the surfactant concentration.

A decrease of the viscosity has not been observed in our system (see Figure 5). At redissolution, the viscosity is already very low and becomes almost independent of the concentration of the added surfactant. The measured values are lower than those obtained for a pure polymer solution, for two possible reasons. First, the added surfactant acts as a salt and screens the repulsion between the polymer charges. The polymer then adopts a less stretched configuration, resulting in a lower viscosity. This effect is illustrated in Figure 5. The replacement of the SDS surfactant by an equivalent concentration of NaCl lowers the viscosity by a factor of 3. A second reason for the viscosity drop could be due to the wrapping of the polymer chains around the micelles, as observed with other systems.<sup>23</sup> Such a conformation might also reduce the hydrodynamic radius of the macromolecules. However, the persistence length of the guar,<sup>39</sup> close to 60 Å, does not favor this structure.

**4.2. Adsorption and Force Profiles.** We first examine the force profiles between the preadsorbed guar layers in pure water solution (i.e., surfactant-free). Figure 7 shows the force profile obtained with the G14 polymer. As already mentioned, no hysteresis, or irreversibility, is observed between measurements performed on approaching or separating the surfaces. Successive runs also give reproducible profiles. Such superposition indicates that the compression does not disturb the adsorbed polymer layer and that our measurements were performed at constant surface coverage. The shape of the force profile displayed in Figure 7 is in qualitative agreement with the curves measured with the other guar of the series. The

(38) Goddard, I. D.; Leung, P. S. *Colloids Surf.* **1992**, *65*, 211.

(39) Robinson, G.; Ross-Murphy, S. B.; Morris, E. R. *Carbohydr. Res.* **1982**, *107*, 17.

range of the measured forces is, however, dependent on the charge rates: the less charged the polymer, the longer the force range (see below).

Force profiles between surfaces covered with a polyelectrolyte have already been measured.<sup>40–44</sup> Authors have reported that, at high separation, when steric forces are not yet present, an electrostatic repulsion is observed between the charged polymer layers.<sup>42</sup> For our free surfactant solutions, the ionic strength was controlled by the small amount of added salt. The corresponding calculated Debye length is lower than 17 nm. In the semilog plot of the G14 force profile, Figure 7, there is no signature of a characteristic length in this range. Even with the G30 guar, the most charged polymer of the series, we do not observe any electrostatic regime in the recorded force profiles. The intensity of such an interaction seems then below the sensitivity of the SFA.

We ascribe an osmotic origin to the very long range repulsive force measured between adsorbed cationic guar layers. Force profiles with similar shapes and having the same origin have been measured between two surfaces covered with polymers in a good solvent.<sup>45–48</sup>

The interactions between polymers and surfaces can lead to a variety of interfacial structures, depending on the nature of the interaction (attractive or repulsive, short or long range), the number of monomers involved, the chain rigidity, the homogeneity of the surface, and other factors. For neutral polymers and short-range attractions, two different structures can be formed.<sup>49</sup> With homopolymers, when all the monomers are attracted by the surface, a fluffy layer of trains, loops, and tails is formed.<sup>50,51</sup> The polymer concentration is high at the surface and decays over a distance  $R$  of the order of the unperturbed coil dimensions in solution,  $R \sim N^{3/5}$ , where  $N$  is the polymerization index of the chains.<sup>52</sup> For flexible polymers in a good solvent, the concentration profile follows a power law as  $\phi \sim z^{-4/3}$ ,  $z$  being the distance from the surface. This interfacial structure is known as the adsorbed layer.

When nonadsorbing polymers are end-grafted to the surface, at high enough surface densities, the concentration profile decays from the surface as a parabola. The strong excluded volume interactions in these grafted polymer layers, also known as brushes, lead to highly extended chains:<sup>53</sup> the layer thickness scales linearly with molecular weight and can be many times larger than the bulk dimensions of the coil in solution.

When two adsorbed layers are brought into contact, they give rise to a repulsive force,<sup>49–51</sup> provided that no desorption takes place during the experimental time. At large separations, the pressure exerted by the polymer

layers reflects the structure of the homogeneous layer and varies to the power  $-3$  of the surface separation. For smaller distances, the compression flattens the polymer profile and a smaller power of  $-9/4$  is observed in the pressure profile. Note that, in this regime where the average concentration in the gap increases inversely with the distance  $\phi \sim 1/d$ , the SFA acts as a micro-osmometer: the variation of the osmotic pressure with polymer concentration can be directly extracted from the force–distance curve (see below).

The compression profile of grafted layers does not exhibit the  $-3$  regime observed for adsorbed layers. However, after a short rapid increase from zero, the  $-9/4$  regime<sup>49,54</sup> is also observed, indicating a rather homogeneous and uniform layer where the average concentration grows inversely with distance.

In our system, several new factors need to be considered in order to accurately describe the adsorption process. The mica surfaces being nonadsorbing for the neutral guar, adsorption must proceed by electrostatic interactions between the negative charges on the mica surface and the cations of the polymer. Thus, only a finite fraction of the monomers along the polymers are responsible for the attraction, and the situation is somewhat intermediate between the adsorbed and grafted cases. Moreover, both the range and strength of the attractive interaction between the polymers and surface are considerably larger than that for neutral polymer adsorption.

Lacking a precise theoretical prediction for the force profile in our system, we decided to concentrate on the large compression regime, where a power law is observed. To fit our data, we use an expression inspired from the Alexander de Gennes<sup>49</sup> description of polymer brushes, compressed between two plates. As we will see, we find a very good agreement between the exponents of the force profiles and the osmotic pressure measured independently. Such agreement indicates that the cationic guar is adsorbed in a rather compact and uniform layer. Other authors have reached the same conclusion with different adsorbed polymers, especially with high-molecular-weight polymers.<sup>42,55</sup>

The pressure between two polymer brushes of size  $L_0$  adsorbed on parallel plates of separation  $D$  is given by the Alexander de Gennes equation:<sup>49–54</sup>

$$P(D) \approx \frac{k_B T}{s^3} \left[ \left( \frac{2L_0}{D} \right)^x - \left( \frac{D}{2L_0} \right)^{3/4} \right] \quad D < 2L_0 \quad (2)$$

The left-hand term in the brackets describes the osmotic repulsion, which increases with the concentration as  $\phi^x$ . The exponent  $x$  is  $9/4$  for neutral polymers and 1 for a highly charged polyelectrolyte,<sup>56</sup> both in good a solvent. When the concentration in the gap is uniform, this translates into the  $1/D^x$  pressure–distance relation, provided that no desorption takes place. The second contribution arises from an elastic restoring force when the overstretched chains<sup>53</sup> are brought closer to their bulk equilibrium configuration. We only use this term as a convenient cutoff function for the force; the choice of its particular exponent has only a small effect on the determination of  $x$ .

The surface force apparatus allows for a measure of the force–distance profile between two crossed cylindrical surfaces. The Derjaguin approximation<sup>57</sup> relates this force

(40) Luckham, P. F.; Klein, J. *J. Chem. Soc., Faraday Trans. I* **1984**, *80*, 865.

(41) Afshar-Rad, T.; Bailey, A. I.; Luckham, P. F.; MacNaughtan, W.; Chapman, D. *Colloids Surf.* **1987**, *25*, 263.

(42) Kamiyama, Y.; Israelachvili, J. *Macromolecules* **1992**, *25*, 5081.

(43) Dahlgren, M. A. G. Ph.D. Dissertation. Royal Institute of Technology, Stockholm, Sweden, 1995.

(44) Kjellin, U. R. M.; Cleasson, P. M.; Audebert R. *J. Colloids Interface Sci.* **1997**, *190*, 476.

(45) Klein, J. In *Molecular Conformation and Dynamics of Macromolecules in Condensed Systems*; Nagasawa, M., Ed.; Elsevier: Amsterdam, Holland, 1988; p 333.

(46) Luckham, P. F.; Klein, J. *J. Colloid Interface Sci.* **1987**, *117*, 149.

(47) Luckham, P. F.; Klein, J. *Macromolecules* **1985**, *18*, 721.

(48) Tauton, H. J.; Toprakcioglu, C.; Fetters, L. J.; Klein, J. *Macromolecules* **1990**, *23*, 571.

(49) de Gennes, P. G. *Adv. Colloid Interface Sci.* **1987**, *27*, 189.

(50) de Gennes, P. G. *Macromolecules* **1982**, *15*, 492.

(51) de Gennes, P. G. *Macromolecules* **1981**, *14*, 1637.

(52) de Gennes, P. G. *Scaling Concepts in Polymer Physics*; Cornell University Press: Ithaca, NY, 1985.

(53) Alexander, S. *J. Phys. (Paris)* **1977**, *38*, 983.

(54) de Gennes, P. G. *C. R. Hebd. Seances Acad. Sci.* **1985**, *300*, 839.

(55) Luckham, P. F.; Klein, J. *J. Chem. Soc., Faraday Trans.* **1990**, *86*, 1363.

(56) Pincus, P. *Macromolecules* **1991**, *24*, 2912.

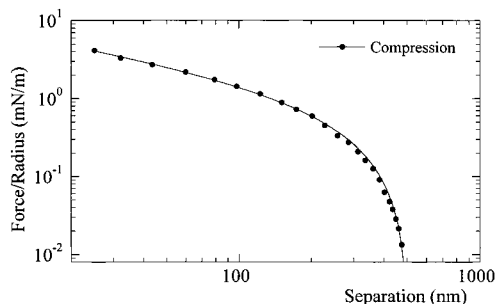


**Figure 11.** log–log force profile between two mica surfaces coated with G14 guar, in the absence of the surfactant (experimental points). The line is the best fit obtained with eq 3, with  $x = 1.6$ .

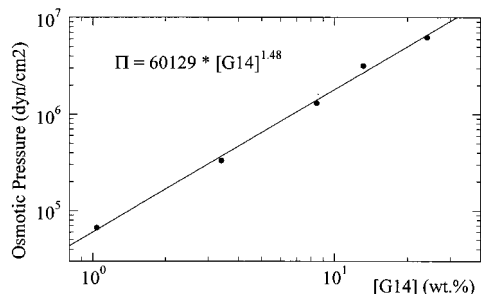


**Figure 12.** Osmotic pressure  $\Pi$  as a function of the G14 concentration. The line is the best fit obtained with a power law.

to the density of interaction free energy between two parallel plates. Hence, after integration of eq 2 we obtain the following modeling force for two curved surfaces:

$$F(D) \cong 2\pi RW(D) = 2\pi R \int P(D) dD \\ \approx \left[ 7 \left( \frac{2L_0}{D} \right)^{x-1} - 4(1-x) \left( \frac{D}{2L_0} \right)^{7/4} + 4(1-x) - 7 \right] \quad (3)$$

In a log–log scale, eq 3 is linear for the short separations where the osmotic contribution is dominant. A similar behavior is seen for the force profiles of any adsorbed cationic guar in the absence of a surfactant. In Figure 11, we present the force profile for G14 and the best fit obtained with  $x = 1.6$ . With identical G14 preadsorbed layers, under similar conditions, the fitting procedure always provides values for  $x$  between 1.5 and 1.6. This value close to  $3/2$  does describe neither a polymer in a good solvent nor a polyelectrolyte solution. We may assume that the experiments were performed under true equilibrium conditions: long relaxation times were allowed between the successive steps of the measurement and different runs give reproducible results. To further test the accuracy of the obtained exponent, we have measured the osmotic pressure of the G14 guar in bulk, for several guar concentrations from 1 to 25 wt % corresponding to the concentration range probed by the SFA (see below). The measurements have been done with dialysis bags using dextran or poly(ethylene glycol) as the stresser. The result, showed in Figure 12, indicates that indeed the osmotic pressure,  $\Pi$ , varies by the power  $3/2$  of the concentration,  $\Pi \sim [\text{G14}]^{3/2}$ . This unusual result will be discussed in a forthcoming paper.

The fitting procedure also provides the range of the steric interaction,  $2L_0$ . The ranges are very long; one has

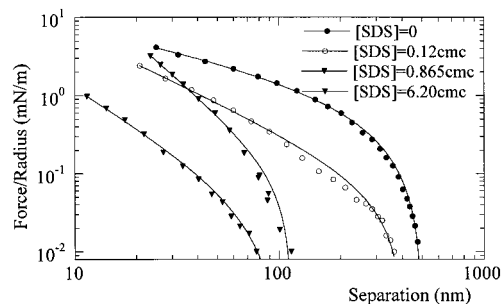


**Figure 13.** log–log force profiles between two mica surfaces coated with G14 guar, in SDS solutions of different concentration. The lines are the best fits obtained with eq 3 with  $x$  as a free parameter.

for instance 900 nm for the G4 polymer, but recall that the molecular weight of these cationic guar may allow such swollen configurations. We have reported in the insert of Figure 8 how  $2L_0$  evolves with the charge density of different studied guar. In the first approximation, the force range seems to follow an algebraic law in respect to the charge ratio; the exponent is roughly equal to  $-0.7 \pm 0.1$ .

We also determined, for the G14 guar, the evolution of the refractive index as a function of the separation between the surfaces. After a refractometric calibration, the average polymer concentration in a noncompressed adsorbed layer of guar is estimated between 1 and 2% in weight. This corresponds to the average polymer concentration when the separation between the two surfaces is 480 nm. For a layer thickness of 240 nm, a 2 wt % concentration corresponds to an adsorbed amount of about 5 mg/m<sup>2</sup>, a large value if compared to the typical amount for an adsorbed neutral polymer (between 0.1 and 1 mg/m<sup>2</sup>) but of the order of surface coverage densities obtained by end-grafting polymers. Adsorption of the same G14 guar has also been studied by using different techniques and different substrates. These measurements obtained with a quartz microbalance,<sup>58</sup> by total internal reflection fluorescence<sup>59</sup> and absorption spectroscopy,<sup>60</sup> indicate values consistent with 5 mg/m<sup>2</sup> or even larger.

We now discuss the evolution of force profiles when the surfactant is gradually added to the water solution. Binding of the anionic surfactant to the cationic guar leads to the electroneutralization in the first stage. The polyelectrolyte becomes a regular polymer and the exponent  $x$  of the modeling force (3) turns out to be  $9/4$ . However, according to the bulk-phase behavior, beyond some surfactant concentration the solution becomes a poor solvent for the surfactant/guar complex when the macromolecules undergo hydrophobic attraction and shrink progressively into a gel. In a poor solvent the exponent  $x$  should increase up to 3 and more.<sup>61–64</sup> We expect thus that steeper force profiles combined with the shrinkage of the adsorbed layer thickness. Up to high surfactant concentrations, eq 3 fits reasonably well with the measured force profiles as illustrated in Figure 13. For the G14 guar, Figure 14, the exponent  $x$  is found to increase from

(58) Anthony, O.; Vanderlyck, K., unpublished results.

(59) Anthony, O.; Santore, M. M., unpublished results.

(60) Patterson, J.; Russel, W. B.; Anthony, O. To be submitted for publication.

(61) Doi, M.; Edwards, S. F. *The Theory of Polymer Dynamics*; Clarendon Press: Oxford, U.K., 1986.

(62) Ross, R. S.; Pincus, P. *Macromolecules* **1992**, *25*, 2177.

(63) Borisov, O. V.; Birshtein, T. M.; Zhulina, E. B. *J. Phys. II* **1991**, *1*, 521.

(64) Borisov, O. V.; Zhulina, E. B.; Birshtein, T. M. *Macromolecules* **1994**, *27*, 4795.

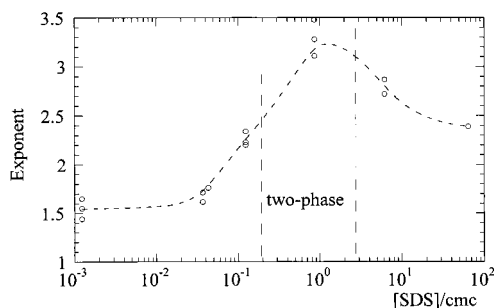


**Figure 14.** Variation of the exponent  $x$  of eq 3 as a function of the SDS concentration.

its initial value of  $3/2$  to a maximum value above 3 for a surfactant concentration corresponding to the two-phase domain of the bulk-phase diagram (Figure 2).

The evolution of the force range also reflects changes in the phase diagram. A reduction of the layer thickness is observed, caused both by the decrease of the charge rate of the polymer (due to the surfactant binding) and also by the hydrophobic attractions between surfactants bound to the polymer. As illustrated by the results for the G14 guar/SDS system, this last effect can be directly related to the increase of the bulk viscosity (Figure 5) in the same surfactant concentration range. The dramatic flattening of the adsorbed layer obtained when 0.865 cmc SDS is added (○, Figure 9) indicates that the system follows the same phase behavior at the interface and in the bulk.

A decrease in the layer thickness is in apparent contradiction to the literature, where a thickness increase has more often been reported<sup>7,8,44</sup> and attributed to the binding of the surfactant onto the polymer layer. In a particular case,<sup>7</sup> the thickness was multiplied by 5 (from 50 to 250 nm for the double layer) upon the addition of  $2 \times 10^{-3}$  M SDS. In those experiments, the addition of SDS has been done with no preliminary rinsing of the nonadsorbed polymer. Therefore, the addition of the surfactant may induce a hydrophobic binding of the free polymer onto the already adsorbed polymer layer when the precipitation line is approached. Therefore, the reported thickness increase is not necessarily related to a change of the conformation of the adsorbed polymer but may be due to a "multilayer" polymer binding. Performing an experiment where we did not remove the free guar of the initial solution has checked this assumption. We then added enough SDS to be in the two-phase region of the phases diagram ( $[SDS] = 0.865$  cmc). The force measurements could not be performed due to a too thick adsorbed layer (about  $10 \mu\text{m}$ ). An additional adsorption of the guar onto the already adsorbed layer has then been induced by the surfactant, reflecting behavior in the bulk-phase diagram.

In conclusion, the modification of the conformation of the polymer at the interface probed by the force profile indicates that the loops formed by the adsorbed polymer behave like solubilized polymer chains and follow a very similar phase behavior, at least in the two first domains in a surfactant concentration.

## 5. Conclusion

The aim of this work was to establish the interrelation between the phase behavior of an oppositely charged polyelectrolyte/surfactant mixture and the structure evolution of the corresponding polyelectrolyte adsorbed and exposed to solutions of the same surfactant. Solutions of cationic guar and the sulfate surfactant have then been studied. We have first determined their phase diagram. These systems behave as usual mixtures of an oppositely charged polymer/surfactant. The solution phase-separates at low surfactant concentrations and the gellike precipitate redissolves at higher surfactant concentrations. Since the neutral backbone of guar is water-soluble, the reduction of the overall charge or charge-reversal mechanism of the chains due to the ionic binding of the surfactant might be dismissed as being at the origin of the coarservation and the redissolution. The demixion originates from an associative mechanism, proceeding by hydrophobic interaction between bound surfactants of different polymer chains. The redissolution of the surfactant/polymer complexes occurs when the surfactant concentration is brought a few times to the cmc. Correlated behaviors are also observed when the polymers are no longer in solution but adsorbed on the surface. Using the SFA, we have shown that the cationic guar adsorb on mica surfaces from free surfactant solutions, in a steady, thick, dense, and uniform layer. The preadsorbed layers of guar shrink when the surfactant is gradually added into the surrounding solution. The shrinkage reaches its maximum when the surfactant concentration belongs to the bulk two-phase concentration range. The force profiles between preadsorbed layers of guar are osmotic in nature and their evolution might be understood in terms of a good solvent becoming a poor solvent when the surfactant concentration is increased. This agrees fully with the bulk-phase behavior. However, when the surfactant concentration is many times the cmc, the adsorbed layers, previously collapsed by the addition of the surfactant, are not reswelled at the surfaces but partially desorbed from them.

In this study, the preadsorbed layers of guar have been exposed to a progressively increasing concentration of surfactant. To get a more complete understanding of such a system, two supplementary studies can be envisaged. The first one consists of collapsing first the preadsorbed layers by adding enough surfactant and then reducing the surfactant concentration. The second study is to perform an adsorption directly from mixtures of a surfactant and polyelectrolyte at concentrations spanning the three domains of the phase diagrams. These two studies are presently underway.

**Acknowledgment.** It is a pleasure for us to thank G. Schorch who has initiated this work and brought us support and interest to realize it.

LA980197X